Inorganic Chemistry

Article

pubs.acs.org/IC

New Supramolecular Au^{I}–Cu^{I} Complex as Potential Luminescent Label for Proteins

D. V. Krupenya, P. A. Snegurov, E. V. Grachova, V. V. Gurzhiy, and S. P. Tunik*

Department of Chemistry, St. Petersburg State University, Universitesky pr. 26, 198504 St. Petersburg, Russia

A. S. Melnikov and P. Yu. Serdobintsev

Department of Physics, St. Petersburg State University, Ulianovskaya st. 3, 198504 St. Petersburg, Russia

E. G. Vlakh, E. S. Sinitsyna, and T. B. Tennikova*

Department of Chemistry, St. Petersburg State University, Universitesky pr. 26, 198504 St. Petersburg, Russia
Institute of Macromolecular Compounds, Russian Academy of Sciences, Bolshoy pr. 31, 199004 St. Petersburg, Russia

Supporting Information

ABSTRACT: A novel supramolecular $[Au_6Cu_2(C_2C_6H_4\text{-}4\text{-}COONC_4H_4O_2)_6(Ph_2PC_6H_4PPh_2)_3](PF_6)_2$ complex functionalized with a succinimide ester alkynyl substituent has been synthesized and characterized using X-ray crystallography, mass spectrometry, and NMR spectroscopy. Like the other complexes of this class, it demonstrates bright emission in acetone and dichloromethane solutions with the excited state lifetime in a microsecond domain. This complex readily reacts with a surface amine group of proteins/enzymes (human serum albumin (HSA), rabbit anti-HSA antibodies, soybean trypsin inhibitor, and α-chymotrypsin) to give covalent conjugates, which contain up to five molecules of the luminescent label bound to the biomolecule. The conjugates keep a high level of the phosphorescent label emission, but in contrast to the parent complex molecule, display excellent solubility and high stability in physiological media. Investigation of the biological activity of the conjugates also showed that the specific structure of the biomolecules remained nearly unchanged upon bonding with the label, which is indicative of a very prospective of the conjugates application in biomolecular detection.

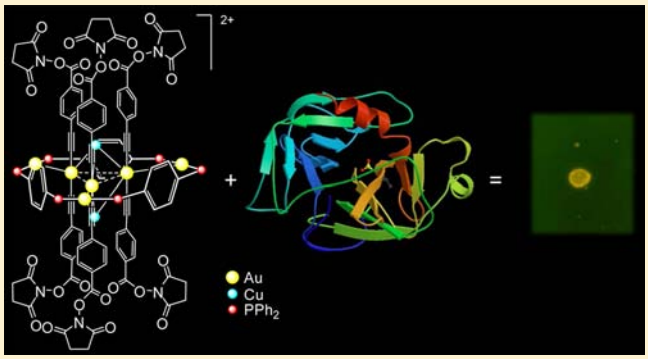

INTRODUCTION

Organometallic complexes based on transition metals are now playing an important role in many biomedical applications, such as anticancer drugs, bioimaging labels, and sensors for various biomolecules.[1−5] In the latter two applications, the transition metal complexes render two evident advantages over widely used fluorescent organic compounds, namely, (1) easily tunable absorption−emission characteristics of chromophoric molecules via variations in ligand environment and the nature of coordinating metal ion and (2) the opportunity to use a time-gated (time-resolved) signal detection procedure that allows substantial increasing of the sensitivity of analysis due to cutoff the autofluorescence of organic background in both in vivo and in vitro experiments.[4−6] It has to be also mentioned that, in many cases, the coordination compounds display higher photostability, which permits continuous monitoring of system properties, as well as pulse-acquisition measurements with enhanced signal-to-noise ratios. However, along with the advantages mentioned above, the metal complexes often suffer low solubility and poor stability in physiological media because of the hydrophobic nature of the ligand environment, which also affects the transport properties of labels and their distribution in biological samples under experimental study. To make these compounds biocompatible and to increase their cellular uptake, as well as their selectivity with respect to certain cells and tissues, the preparation of covalent[7−13] or noncovalent[14−20] conjugates of transition metal complexes with peptides and proteins (HSA, BSA) is commonly used. It was established that the adducts of HSA with luminescent platinum[17] and terbium[19] complexes displayed a strong dependence of luminescence intensity on association with protein that makes possible the application of these compounds as HSA sensors of strong selectivity. The covalent bonding of a

Received: June 25, 2013
Published: October 17, 2013

   dx.doi.org/10.1021/ic401569n | Inorg. Chem. 2013, 52, 12521−12528

wide range of bio-objects with luminescent coordination compounds can be accomplished using the reactions of surface amino groups[4,11−13,21] or by sulfhydryl functionality of cysteine residues[9] of biomolecules with corresponding reactive groups (isothiocyanate, carboxyl, aldehyde, and iodoacetamide) attached to one of the ligands in a complex coordination sphere. In contrast to initial organometallic complexes, the resulting conjugates display high solubility and stability in physiological media, keeping the emission characteristics of labels at an appreciable level. It is worth noting that, in many cases, the conjugates also show extremely selective affinity to certain bio-objects,[7] which is determined by the nature of the biological component of a formed aggregate. This makes it possible to use these conjugates as prospective luminescent labels for bioimaging and as extremely specific reagents to stain cellular organelles. However, it is well-known that phosphorescent labels suffer from luminescence quenching by molecular oxygen due to triplet nature of the excited state, which may suppress the emission by an order of magnitude. To minimize this quenching effect, it is necessary to remove oxygen from analyte, which makes the corresponding protocol time and reagent consuming.

In our recent publications, we described synthesis and characterization of a series of coinage metal heterometallic complexes,[22−24] which displayed extremely high phosphorescence under single and double quantum excitation along with unusually weak oxygen quenching. The combination of these properties made possible the successful application of these complexes for cell staining,[25] thus demonstrating the prospects for further applications of these compounds in bioimaging. Well-elaborated synthetic protocols and stability of reaction products made possible the easy functionalization of the ligand environment[22,26,27] in complexes studied through insertion of various substituents into alkynyl ligands, which substantially broadens the areas of application.

In the present paper, we describe the synthesis and characterization of a gold−copper supramolecular complex functionalized with reactive succinimide ester groups and its conjugation with a series of proteins/enzymes via covalent bond formation. Photophysical properties of the initial complex and its conjugates were also studied in organic and water solutions. Biological activity of the conjugates and the original proteins were compared to display insignificant denaturation of conjugated biomolecules.

EXPERIMENTAL PROCEDURES

Material and Reagents. Tetrahydrothiophene (THT), *N*-hydroxysuccinimide, *N*,*N*′-dicyclohexylcarbodiimide (DCCI), human serum albumin (HSA), rabbit anti-HSA antibodies, α-chymotrypsin from bovine pancreas (ACHT), soybean trypsin inhibitor (SBTI), trypsin from bovine pancreas, *N*-benzoyl-L-tyrosine ethyl ester (BTEE), and *N*-benzoyl-L-arginine *p*-nitroanilide hydrochloride (BAPNA) were purchased from Sigma-Aldrich. 1,4-Bis-(diphenylphosphino)benzene (dppb),[28] [Au(THT)Cl],[29] and [Cu(NCMe)$_4$]PF$_6$[30] were synthesized according to published procedures. Acetone, dimethyl sulfoxide, and methanol were purchased from Vecton. All salts used for the preparation of buffer solutions were produced by Fluka and Sigma-Aldrich and had an analytical grade of purity. Before use, all buffers were filtered with the use of membranes with a pore diameter of 0.45 μm (Millipore). Vivaspin 500 concentrators (10 kDa) by Sartorius or a glass column of 280 × 5 mm i.d. packed with Sephadex G-100 (Pharmacia) was applied to purify the bioconjugates from the excess of the luminescent complex (label).

Instrumentation. To purify the bioconjugates by gel-filtration, the low pressure chromatographic system consisted of a Masterflex console drive Easy-Load II Model 77201-60 pump (Cole-Parmer Instrument Company) and a 2138 Uvicord S UV detector (LKB). For purification of bioconjugates by ultrafiltration, a SIGMA 2-16P centrifuge (SIGMA Laborzentrifugen GmbH) was applied. The lyophilization of bioconjugates was performed using FreeZone1 (LABCONCO). The determination of absorbance of the analyzed solutions was performed using an UVmini-1240 UV−vis spectrometer (Shimadzu). The in-solution ^{1}H and ^{31}P NMR spectra were recorded on a Bruker DPX 300 spectrometer. Mass spectra were measured on a Bruker APEX-Qe ESI FT-ICR instrument. Elemental microanalyses were carried out using EuroVector3000 (EuroVector Factory). A DTL-399QT DPPS pulse laser (wavelength 351 nm, pulse energy 50 μJ, repetition rate 1 kHz, pulse width 6 ns; Laser Export, Russia) was used to pump luminescence. A Tektronix TDS3014B digital oscilloscope (bandwidth 100 MHz; Tektronix), a MUM monochromator (interval of wavelengths, 10 nm; LOMO), and a photomultiplier tube (Hamamatsu) were used for lifetime measurements. Emission spectra were recorded using an HR2000 spectrometer (Ocean Optics, Inc.). A LS-1-CAL halogen lamp and a DH2000 deuterium lamp (Ocean Optics, Inc.) were used to calibrate the absolute spectral response of the spectral system in the 200−1100 nm range. Absorption spectra were measured on a Varian Cary 50 spectrophotometer (Varian). Excitation spectra were recorded on a Varian Cary Eclipse spectrofluorometer (Varian).

Synthesis. *2,5-Dioxopyrrolidin-1-yl 4-Ethynylbenzoate.* 4-Ethynylbenzoic acid (277 mg, 1.9 mmol) and *N*-hydroxysuccinimide (240 mg, 2.1 mmol) were dissolved in THF (5 mL), and a solution of DCCI (433 mg, 2.1 mmol) in THF (5 mL) was added. The reaction mixture was stirred for 1 h. A white precipitate was removed by filtration, and a solution was separated by normal phase column chromatography using silicagel as a stationary phase and a mixture of hexane and ethyl acetate (1:1 v/v) as a mobile phase. Yield: 254 mg (55%). ^{1}H NMR ($CDCl_3$, RT): δ 8.11 (d, $^3J_{HH}$ = 8.3 Hz, 2H, Ph), 7.63 (d, $^3J_{HH}$ = 8.3 Hz, 2H, Ph), 2.93 (s, 4H, CH_2CH_2).

[AuC$_2$C$_6$H$_4$-4-COONC$_4$H$_4$O$_2$]$_n$. [Au(THT)Cl] (145 mg, 0.45 mmol) was suspended in a solution of 2,5-dioxopyrrolidin-1-yl 4-ethynylbenzoate (137 mg, 0.56 mmol) in THF (2 mL), and a few drops of Et_3N were added. The reaction mixture was stirred for 1 h in the dark. The precipitate was collected by centrifugation and was twice rinsed with a water−ethanol mixture, ethanol, and pentane and was dried under vacuum. Yield: 188 mg (95%). The polymer obtained was used in the synthesis without further purification.

*[(AuC$_2$C$_6$H$_4$-4-COONC$_4$H$_4$O$_2$)$_2$(PPh$_2$C$_6$H$_4$PPh$_2$)] (**1**).* Dppb (67 mg, 0.15 mmol) and [AuC$_2$C$_6$H$_4$-4-COONC$_4$H$_4$O$_2$]$_n$ (140 mg, 0.32 mmol) were dissolved in dichloromethane (5 mL). The reaction mixture was stirred for 30 min, and toluene (2.5 mL) was added. The solution was passed through a neutral alumogel plug and evaporated to produce a dry white crystalline powder. Yield: 130 mg (65%). ^{31}P{^{1}H} NMR ($CDCl_3$, RT): δ 43.3 (s, 2P). ^{1}H NMR ($CDCl_3$, RT): δ 8.04 (d, $^3J_{HH}$ = 8.3 Hz, 4H, $C_2C_6H_4$), 7.53−7.64 (m, 28H), 2.91 (s, 8H, CH_2CH_2).

*[Au$_6$Cu$_2$(C$_2$C$_6$H$_4$-4-COONC$_4$H$_4$O$_2$)$_6$(Ph$_2$PC$_6$H$_4$PPh$_2$)$_3$](PF$_6$)$_2$ (**2**).* Compound **1** (44 mg, 0.033 mmol) was dissolved in CH_2Cl_2 (3 mL), and [Cu(NCMe)$_4$]PF$_6$ (8.3 mg, 0.022 mmol) was added. The reaction mixture was stirred for 1 h, and the yellow-orange solution was filtered through Celite, evaporated to dry product, and recrystallized by gas-phase diffusion of pentane into an acetone solution. Yield: 39 mg (84%). ESI-MS: m/z = 2050.67 $[M]^{2+}$ (calcd 2050.67). ^{31}P{^{1}H} NMR (acetone-d_6, RT): δ 44.4 (s, 6P), −144.8 (sept, $^1J_{PF}$ = 707 Hz, 2P, PF_6). ^{1}H NMR (acetone-d_6, RT): δ diphosphine, 8.00 (dm (ABXX′), $^3J_{HH}$ = 7.2 Hz, $^3J_{PH}$ = 13 Hz, 24H, ortho-H), 7.85 (m, 12H, {P−C$_6$H$_4$−P}), 7.67 (t, $^3J_{HH}$ = 7.4 Hz, 12H, para-H), 7.51 (dd, $^3J_{HH}$ = 7.4 and 7.2 Hz, 24H, meta-H); {Au(C$_2$C$_6$H$_4$-4-COONC$_4$H$_4$O$_2$}, 7.56 (d, $^3J_{HH}$ = 8.3 Hz, 12H, C$_6$H$_4$), 7.05 (d, $^3J_{HH}$ = 8.3 Hz, 12H, C$_6$H$_4$), 2.95 (s, 24H, CH_2CH_2).

X-ray Crystal Structure Analysis. For the single-crystal X-ray diffraction experiment, the crystal of **2** obtained was fixed on a micromount and placed on a Bruker Kappa APEX II DUO

Scheme 1. Synthesis of Complex 2

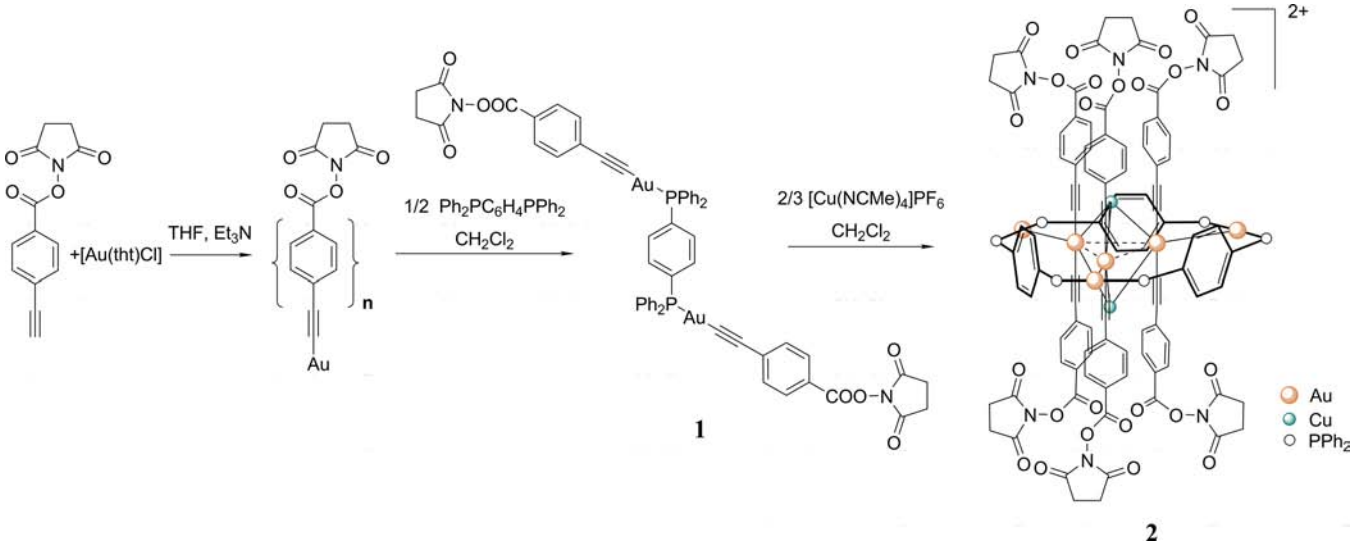

diffractometer. The measurement was carried out at 100 K using monochromated microfocused Mo Kα radiation. The crystal of **2** was very weakly diffracting, thus the resolution of the data set results in the rather low 2θ range of 1.68−45.02°. Additionally, the structure has been analyzed by direct methods using the SHELX-97 program[31] incorporated in the OLEX2 program package.[32] The positions of H atoms were modeled using the "riding" model. Absorbance correction was applied using the SADABS program.[33] Crystallographic data for the compound **2** are presented in Table S1 (Supporting Information). Supplementary crystallographic data for this paper have been deposited at Cambridge Crystallographic Data Centre (CCDC 923479) and can be accessed at www.ccdc.cam.ac.uk/data_request/cif.

Bioconjugate Synthesis. To synthesize the "protein/label" bioconjugates, three model proteins, namely SBTI, HSA, and anti-HSA antibodies, were chosen. A sodium phosphate buffer (0.01 M, pH 7.5 and 8.0) and a 0.01 M sodium borate buffer (pH 8.4) were used as reaction media. The reaction time was varied from 15 to 120 min. The protein/luminescent complex molar ratio was changed in a range from 1:1 up to 1:10 depending on protein molecular mass. The concentrations of initial compounds used in bioconjugation were the following: proteins, 1 mg/mL in buffer; luminescent marker (organometallic complex), 8 mg/mL in acetone. The conjugates were prepared by the addition of corresponding aliquot of the complex solution to the protein solution. The reaction mixture was stirred and incubated in the dark at 22 °C. The monitoring of product formation was fulfilled by a gel-filtration method using a glass column (280 × 5 mm i.d.) packed with swollen Sephadex G-100. The amount of loaded sample was equal to 0.1 mL; the filtration flow rate was 0.25 mL/min, and the detection of all components was performed photometrically at a wavelength of 280 nm.

To establish the protein/label ratio, the fraction corresponding to the unbound organometallic complex was collected and its amount was measured photometrically at 265 nm. The amount of conjugated label was calculated as the difference between those used in the synthesis and those separated after the reaction completion.

ACHT Conjugate Preparation and Study of Its Activity. To determine the specific activity labeled enzyme, the bioconjugates were prepared using protein/luminescent complex molar ratios equal to 1:3 and 1:5. A sodium borate buffer (0.01 M, pH 8.4) was used as the reaction medium. The reaction time was 60 min. After the reaction was complete, the label excess was separated via ultrafiltration through a 10 kDa membrane. The determination of activity of the enzyme bound to the luminescent complex was carried out using BTEE as specific low molecular mass substrate, and the protocol was published elsewhere.[34] The substrate concentrations were changed in the range 0.01−0.25 mg/mL; the amount of conjugated enzyme used for biocatalytical assay was constant and equal to 0.025 mg. The time of reaction was 1 min. The calculation of the kinetic parameters was carried out using a graphical method based on plotting of the dependence of hydrolysis velocity versus the substrate concentration (Michaelis−Menten plot) and further linearization of resulted graph in inversed coordinates (Lineweaver−Burk plot).

SBTI Conjugate Preparation and Study of Its Inhibitory Ability. The conjugate of SBTI with the luminescent complex was obtained using a molar ratio of protein and label equal to 1:3. Other conditions were the same as described earlier for the reaction of ACHT conjugation. Hydrolysis of BAPNA by trypsin was carried out in the presence of native SBTI or its conjugate with the luminescent complex. To determine the inhibition constants, different amounts of inhibitor were added to an invariable amount of trypsin (0.025 mg per 3 mL of reaction solution) at three different substrate concentrations. The SBTI:trypsin ratio used in the reaction mixture was equal to 1:10, 1:5, 1:3.3, and 1:2.5. SBTI was added to the enzyme solution in 0.05 M Tris−HCl buffer, pH 8.0, containing 0.005 mol/L of $CaCl_2$, to get, in sum, 2.3 mL of reactive solution, which was incubated for 10 min at 22 °C. The corresponding aliquot of BAPNA solution in the same buffer was then added to the reaction mixture to obtain 3 mL of the solution and total substrate concentration equal to 0.1, 0.3, and 0.5 mM. The reaction of hydrolysis was performed for 10 min; the reaction product (*p*-nitrophenol) was detected with the use of UV−vis spectroscopy at a wavelength of 410 nm. The reciprocal velocities ($1/v$) versus inhibitor concentration [I] for each substrate concentration were plotted (Dixon's plot) to obtain the inhibition constant as the intersection of three linear graphs.

RESULTS AND DISCUSSION

Synthesis and Structural Characterization of Au^{I}−Cu^{I} Supramolecular Complex. The 2,5-dioxopyrrolidin-1-yl 4-ethynylbenzoate ligand was synthesized by modified published method[35] using DCCI as a coupling reagent instead of *N*,*N*,*N*′,*N*′-tetramethyl-*O*-(*N*-succinimidyl)uronium tetrafluoroborate applied earlier to insert the reactive succinimide group, which was widely used to bind various labels to biomolecules through the surface amino groups of latters.[36]

The heterometallic luminescent complex **2** was obtained using the standard procedure described earlier for these type of complexes[22,37] (Scheme 1). At the first step, the alkynyl−gold polymer complex was obtained. Usually this reaction is carried out in an acetone−water media, but in this case, the reaction with triethylamine as a base proceeds in THF to avoid

dx.doi.org/10.1021/ic401569n | *Inorg. Chem.* 2013, 52, 12521−12528

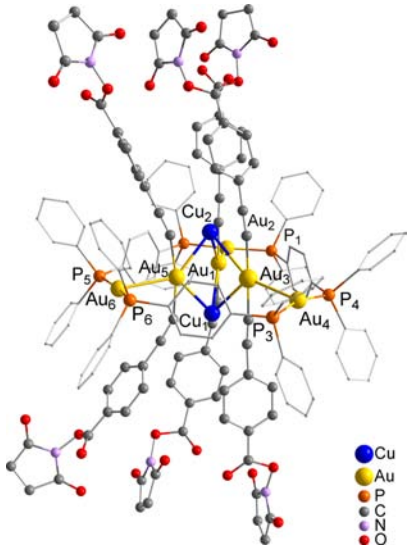

Figure 1. Molecular view of the dication **2**. Hydrogen atoms are omitted for clarity. Selected interatomic distances (Å): Au(1)−Au(3) 3.433(1), Au(1)−Au(5) 3.370(1), Au(3)−Au(5) 3.430(1), Au(1)−Au(2) 2.841(1), Au(3)−Au(4) 2.907(1), Au(5)−Au(6) 2.884(1), Cu(1)−Au(1) 2.888(3), Cu(1)−Au(3) 2.867(3), Cu(1)−Au(5) 2.683(2), Cu(2)−Au(1) 2.709(2), Cu(2)−Au(3) 2.975(2), Cu(2)−Au(5) 2.720(3), Au(2)−P(1) 2.315(6), Au(2)−P(2) 2.302(6), Au(4)−P(3) 2.323(5), Au(4)−P(4) 2.314(5), Au(6)−P(5) 2.321(5), Au(6)−P(6) 2.321(5).

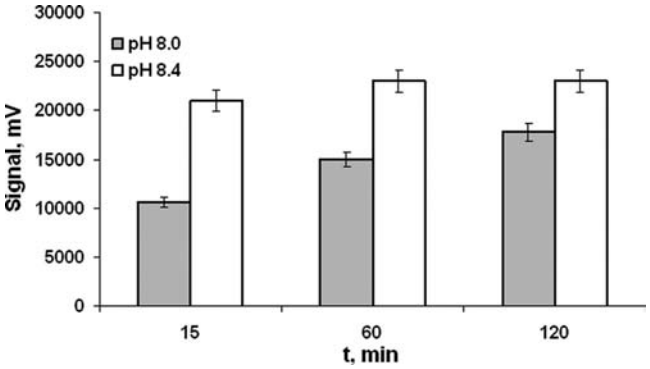

Figure 2. Dependence of bioconjugate formation on experimental conditions: pH and reaction time.

Table 1. Effect of Protein-to-Metal Organic Complex onto Amount of Conjugated Luminescent Label[a]

protein	initial mole ratio protein/metal organic complex	amount of conjugated metal organic complex, %	calculated mole ratio protein/metal organic complex
SBTI	1:3	42	1.0:1.3
SBTI	1:5	38	1.0:1.9
HSA	1:3	42	1.0:1.3
HSA	1:5	42	1.0:2.1
anti-HSA antibody	1:5	51	1.0:2.6
anti-HSA antibody	1:7	49	1.0:3.4
anti-HSA antibody	1:10	48	1.0:4.8

[a]Conditions: reaction media, −0.1 M sodium borate buffer, pH 8.4; reaction time, −60 min, UV detection at 265 nm.

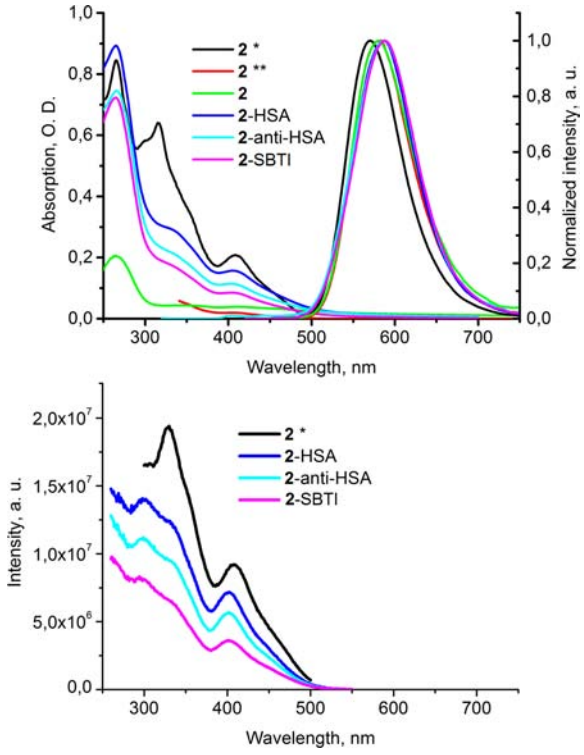

Figure 3. Absorption and emission (top) and excitation (bottom) spectra of **2** and its conjugates in borate buffer (*in CH_2Cl_2; **in acetone), 25 °C, λ_{ex} = 400 nm.

Table 2. Photophysical Properties of 2 and Its Conjugates in Dichloromethane, Acetone, and Sodium Borate Buffer, 25 °C, λ_{ex} = 400 nm

	solvent	λ_{abs}, nm	λ_{ex}, nm	λ_{em}, nm	τ, μs[a]
2	CH_2Cl_2	265, 300 sh, 317, 350sh, 409	330, 350 sh, 408	570	3.3
2	acetone	353 sh, 408	331, 414	580	3.0
2	borate buffer	265, 348, 412	300, 330, 403	580	0.5 (36%), 3.4 (64%)
2−HSA	borate buffer	265, 340 sh, 405	300, 330 sh, 402	586	0.5 (46%), 2.5 (54%)
2−anti-HSA antibody	borate buffer	266, 340 sh, 403	300, 330 sh, 402	587	0.6 (42%), 2.8 (58%)
2−SBTI	borate buffer	265, 340 sh, 404	300, 330 sh, 402	587	0.5 (48%), 2.4 (52%)

[a]Relative contribution of the decay exponents are given in parentheses.

hydrolysis of the succinimide ester functionality. The further reaction with the diphosphine ligand affords the digold complex **1**. The addition of a stoichiometric amount of $[Cu(NCMe)_4]$-PF_6 to a solution of **1** in dichloromethane results in formation of the target complex **2**.

Compounds **1** and **2** were characterized by the ^1H and ^{31}P NMR. The ESI mass-spectrum of **2** displays the signal of the $[Au_6Cu_2(C_2C_6H_4\text{-}4\text{-}COONC_4H_4O_2)_6(Ph_2PC_6H_4PPh_2)_3]^{2+}$ dication according to the proposed stoichiometry of the final reaction product. The crystal structure of complex **2** was revealed by the X-ray diffraction study, and the structural plot of this molecule is given in Figures 1 and S1 (Supporting Information).

dx.doi.org/10.1021/ic401569n | *Inorg. Chem.* 2013, 52, 12521−12528

Table 3. Effect of the Covalent Conjugation of Obtained Metal Organic Cluster Complex with α-Chymotrypsin on Biological Properties of Enzyme

form of biocatalyst	reaction ratio of protein/label	K_M, mM	specific activity, μmol·min^{-1}·mg^{-1}
native ACHT		0.38 ± 0.02	55.8 ± 2.5
2–ACHT	1:3	0.31 ± 0.02	31.9 ± 1.6
2–ACHT	1:5	0.30 ± 0.01	20.5 ± 1.0

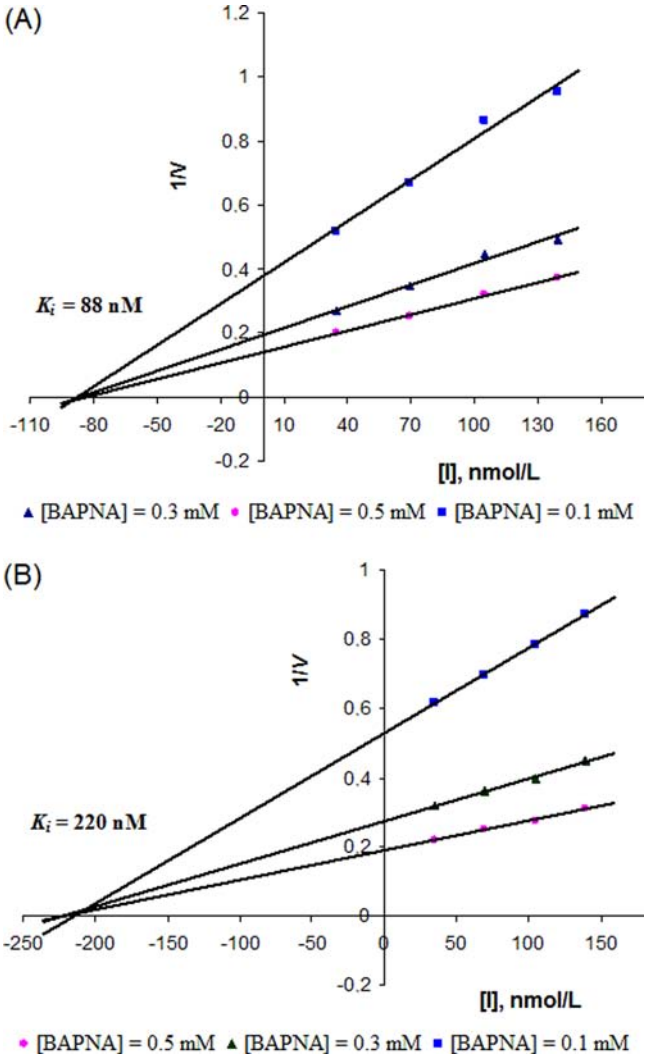

Figure 4. Dixon's plots of trypsin inhibition by native SBTI (A) and its conjugate with organometallic complex (B).

Similar to the previously characterized gold–copper complexes with the same structural motif,[22,26,38,39] the compound consists of the central $[Cu_2(RC_2AuC_2R)_3]^-$ anionic cluster wrapped about by the $[Au_3(PP)_3]^{3+}$ "belt". The six gold atoms of the metal skeleton are located nearly in a single plane, with two copper atoms being above and below the center of the equilateral Au^I triangle. The copper ions are π-coordinated to the triple bonds of the $\{RC_2AuC_2R\}$ fragments and bound to three central gold atoms by metallophilic interactions. The Au–Au contacts between "belt" and central core and Au–Cu contacts in **2** fall in the ranges 2.841–2.907 and 2.683–2.975 Å, which match well the values found earlier for the related bimetallic compounds.[22,26,39–42] The Au–Au contacts inside the cluster core are longer and fall in the range 3.370–3.433 Å, which is indicative a weak aurophilic interaction.

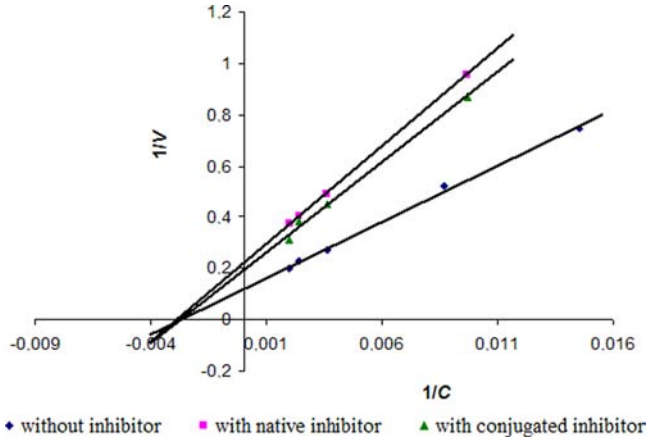

Figure 5. Lineweaver–Burk plots for enzyme catalyzed hydrolysis of BAPNA without inhibitor, in presence of native and conjugated SBTI.

The ^{31}P and ^1H NMR spectra of gold–copper structural relatives of **2** containing various substituents in the alkynyl ligands were described in detail in our previous works.[22,38] Positions, multiplicity, coupling constants, and relative intensity of the signals in the ^{31}P and ^1H NMR spectra of **2** are nearly identical to those found early for the congeners containing different alkynyl substituents.[22,38] The ESI mass spectrum of **2** (Figure S2, Supporting Information) displays a signal of doubly charged cation at m/z 2050.67, the isotopic pattern of which completely fits the stoichiometry of the $[Au_6Cu_2(C_2C_6H_4\text{-}4\text{-}COONC_4H_4O_2)_6(Ph_2PC_6H_4PPh_2)_3]^{2+}$ molecular ion. These observations clearly show that the structure of **2** found in solid state remains unchanged in solution.

Synthesis of Bioconjugates. The succinimide activated ester groups of synthesized luminescent complex **2** allows for direct conjugation with the biomolecules bearing reactive amino groups (for example, proteins) that makes possible the formation of strong conjugates through covalent amide bonds. This reaction is widely used for the synthesis of bioconjugates of different natures.[36,43] In addition to the fast covalent binding, the activated esters are unstable in aqueous solutions at relatively alkaline pH and can be removed at a conjugation reaction by means of hydrolysis. This process represents an additional advantage because it allows avoiding side reactions of excess succinimide groups at the further stages.

It is well-known that optimal pH for the reaction of amine-bearing compounds with organic dyes containing succinimide ester groups lies in the range 8.0–8.4.[36] The pH of buffer, reaction time, and the protein-to-label ratio were varied to establish the optimal conditions for conjugation of a few proteins with complex **2** (luminescent label). Trypsin inhibitor (20 100), human serum albumin (66 400), and anti-HSA antibody (150 000) were used as model proteins at conjugate construction. The separation of the bioconjugates obtained from unbound luminescent label was carried out by gel-filtration using a Sephadex G-100 column. As expected, the reaction was found to be dependent on pH (Figure 2).

dx.doi.org/10.1021/ic401569n | Inorg. Chem. 2013, 52, 12521–12528

Table 4. Effect of Inhibition on Trypsin Activity for BAPNA Hydrolysis[a]

BAPNA trypsinolysis	K_M, mM	specific activity, μmol·min^{-1}·mg^{-1}
without inhibition	0.37 ± 0.02	1.01 ± 0.04
in presence of native SBTI	0.34 ± 0.01	0.54 ± 0.02
in presence of **2**−SBTI	0.36 ± 0.02	0.62 ± 0.02

[a]Conditions: the reaction (molar) ratio SBTI/metal organic complex was equal to 1:3; the ratio trypsin to SBTI was 1.00:0.45.

Moreover, the reaction velocity at pH 8.4 was sufficiently higher and the most bioconjugates were formed in 15 min, whereas the maximum concentration of a product was reached in 60 min. This result is in a good agreement with well-known reactivity of low molecular mass organic succinimide esters.[36]

The effect of the protein-to-luminophore ratio on conjugation reaction was explored using proteins of different molecular masses and different excess of the organometallic complex. Obviously, the smaller molecular mass of a protein, the less amounts of label can be bound without risk of distortion of the biomolecule native structure. Taken into account this consideration, as well as a large size of the luminescent labels, the initial protein/label ratio did not exceed 1:5 in the cases of conjugation with SBTI and HSA. At the same time, for such big molecules as antibodies, this ratio was increased to 1:10. The data given in Table 1 indicate that the amount of organometallic complex bound to the protein falls in the range of 38−51% of initial quantity.

Photophysical Properties. Absorption, excitation, and emission spectra of **2** and its conjugates with HSA, anti-HSA, and SBTI are shown in Figure 3. The photophysical characteristics are presented in Table 2. Absorption spectra of **2** in dichloromethane and acetone looks very similar to the $\{Au_6Cu_2\}$ "rods-in-belt" congeners[22,44] reported earlier.

The long wavelength absorption band at 409 nm can be analogously assigned to $\{Au_6Cu_2\}$ intracore transitions, whereas the absorption at 317 and 265 nm are related to the electronic transitions from σ(Au—P) to π^*(C≡CR) orbital and the intraligand $\pi \rightarrow \pi^*$ (C≡CR) transitions, respectively.[22] Compound **2** is strongly emissive being dissolved in dichloromethane and acetone with emission maxima centered at 570 and 580 nm, respectively.

The excited state is characterized by single exponential decay with the lifetime in a microsecond domain. In borate buffer (λ_{em} 580 nm), compound **2** demonstrates double exponential decay: one component is similar to that observed in organic media, whereas the other shows substantially shorter lifetime. The component with a short lifetime originates very probably from the interaction of **2** with water molecules that results in the appearance of another channel for excited state decay. The conjugates of **2** with proteins also displayed moderate orange emission with the further 6−7 nm (∼190 cm^{-1}) red shift of emission maximum comparatively to the characteristics measured in the buffers. Similarly to photophysical behavior of **2** in aqueous solution, the conjugates showed double exponential decay with almost equal contributions of shorter (0.5−0.6 μs) and longer (2.4−2.8 μs) components. It is worth mentioning that all but one experiment was done in aerated solutions. For the sake of comparison, the intensity of the emission of the **2**−HSA conjugate was measured both in degassed (purging with argon for 15 min) and in aerated solutions. Quite expectedly, the intensity of emission displayed slight variation below the limit of experiment uncertainty (Figure S3, Supporting Information), which is indicative of negligible oxygen quenching of emission. The excitation spectra of the studied organometallic complex and its bioconjugates are very similar and fit well the absorption spectra of the corresponding species.

Study of Biological Activity of Fluorescent Protein/Label Conjugates. There are many papers presenting the synthesis of protein/metal complex conjugates;[7−20] however, to the best of our knowledge, none of them give comparative quantitative estimations of their bioactivity. The traditional fluorescent organic dyes applied to the labels to detect different kinds of biomolecules usually represent the chemical substances with molecular masses below 1500. The molecular mass of the studied luminescent complex is at least 2.5 times higher. It was reasonable to presume that such big molecular fragments covalently bound to the protein macromolecule could change its active conformation and, therefore, influence the biological properties of the labeled biomolecule. Besides the possible conformational distortions caused by conjugation, the steric limitations generated by nanosized luminescent complex may also affect the interaction between two affinity macromolecules. Obviously, the biological properties of small proteins are much more sensitive to a covalent attachment of rather large labels due to a possible appearance of steric hindrance. To investigate the impact of a conjugation of small enough proteins with studied luminescent label on their biological activity, the properties of labeled α-chymotrypsin (ACHT) and soybean trypsin inhibitor (SBTI) were studied. The comparison of biological activity of native and conjugated proteins allowed evaluation the effect of attached luminescent label.

It is well-known that enzymes represent one of the most labile and sensitive group of protein macromolecules. To compare the behavior of native and labeled ACHT at biocatalytic process, the specific low molecular mass substrate, namely, *N*-benzoyl-L-tyrosine ethyl ester (BTEE), was applied. Table 3 summarizes the results on Michaelis−Menten constants (K_M) and specific activity (A_{sp}) of native ACHT and its conjugate with the organometallic complex **2**. The K_M values for bioconjugates prepared with different ACHT/label ratios appeared to be very close to that determined for native ACHT. The results obtained means that the enzyme-to-substrate affinity, as well as a thermodynamic strength of specific complexes, is not affected by conjugation with rather large labels. At the same time, the increase of the ACHT/label ratio displays a visible decrease of enzyme activity, which represents the maximum reaction rate normalized to the one mg of the enzyme. The reduction of the specific enzyme activity by 1.7 times was detected when the starting enzyme-to-label ratio was equal to 1:3. The decrease of this ratio to 1:5 results in 2.7 times reduction of ACHT activity. These observations can be related to partial distortion of a native enzyme conformation due to covalent binding to the label. A similar trend was also observed for the immobilized enzymes.[34,45,46]

To evaluate the effect of protein conjugation with the organometallic label on a specific protein−protein interaction, the model affinity pair trypsin−trypsin inhibitor was chosen. Trypsin inhibitor is a protein that reduces the enzymatic

activity of trypsin by means of blockage of corresponding site on a surface of enzyme molecule.[47] To study the effect of protein conjugation on SBTI specific interaction with its natural counterpart (e.g., trypsin), the inhibition constants (K_i) were determined. The dependence of inhibition activity of SBTI was evaluated by measuring the enzyme hydrolytic activity toward its specific substrate, BAPNA. The reaction was studied in systems containing constant concentration of trypsin, a few different concentrations of SBTI, as well as three different substrate concentrations. Similarly to the Michaelis−Menten constant, the inhibition constant (K_i) determined from Dixon's plot (Figure 4) characterizes the strength of the inhibitor−enzyme complex, in other words, the affinity of inhibitor to its enzymatic complement.

It was determined that the inhibition constant calculated for SBTI conjugated with an organometallic label (label-to-enzyme ratio 1:3) appeared to be 2.5 higher than that found for the native inhibitor (220 and 88 nM, respectively). Despite increasing the K_i of the conjugated inhibitor, the determined values of inhibition constants indicate a rather high affinity of tested pairs of proteins (enzyme−inhibitor) in both cases. Thus, it can be concluded that the ability to form the affinity pair is insignificantly affected by the binding of a protein to large luminescent molecule.

The K_M and A_{sp} values obtained from the Lineweaver−Burk plots (Figure 5) for the catalyzed hydrolysis of BAPNA without inhibitor, in presence of native and conjugated SBTI are summarized in Table 4. In all cases, the K_M values of enzyme catalysis were found to be nearly the same. Thus, the addition of inhibitor did not influence the process of the enzyme−substrate complex formation that, in turn, means that the inhibition mechanism can be related to the noncompetitive type.

As it was expected, the inhibitor addition followed the enzyme activity reduction. Because the inhibitor amount was equal to 40% of that of the enzyme, the theoretically predicted residual enzymatic activity was expected to be 60% compared to the activity determined without the inhibitor. Indeed, the remaining trypsin activity in a presence of native SBTI and its conjugate with the luminescent complex was close to 60% for conjugated and nonconjugated inhibitor. Therefore, the effect of the organometallic complex of affinity protein−protein pair formation can be counted as negligible.

CONCLUSIONS

The synthesized supramolecular Au^I−Cu^I complex can be applied as a long-term phosphorescent label for biomolecules, in particular, for proteins of various molecular masses and biological functionalities. Despite a rather large organometallic complex, the formation of its conjugates with the protein of choice did not prevent the specific interaction of latter with affinity partner. The result obtained means that the label can be used in various diagnostics or analytical based on formation of affinity complexes followed by high sensitive detection of target biomolecule using emission signal measurement. The measurement of the emission from the excited triplet state characterized by the lifetime in a microsecond domain makes it possible to decrease the analytical threshold by application of a time gated procedure, which cut off the background fluorescence and considerably increased the signal-to-noise ratio.

ASSOCIATED CONTENT

Supporting Information

X-ray crystallographic data for complex **2** in CIF format, ORTEP view and ESI^+ mass spectrum of **2**, a comparison of emission spectra of **2**−HSA aerated and degassed solutions in PBS. This material is available free of charge via the Internet at http://pubs.acs.org.

AUTHOR INFORMATION

Corresponding Authors

*Prof. Dr. Chem. Sci. S. P. Tunik.

*Prof. Dr. Chem. Sci. T. B. Tennikova. Tel: +7 (812) 3236401. Fax: +7 (812) 3236869. E-mail: tennikova@mail.ru.

Notes

The authors declare no competing financial interest.

ACKNOWLEDGMENTS

The authors greatly appreciate the financial support of St. Petersburg State University research grants 12.39.1048.2012 and 12.37.132.2011, and grants 11-03-92010 as well as 13-00-40342-K/13-04-40342 from the Russian Foundation for Basic Research. The Finnish−Russian collaborative project (strategic funding of the UEF) is also acknowledged. The work was carried out using scientific equipment of the Center of Shared Usage "The analytical center of nano and biotechnologies of SPbSPU" with financial support of Ministry of Education and Science of Russian Federation and "Center of Optical and Laser Methods for Material Investigation", St. Petersburg State University. NMR studies were performed at the Centre for Magnetic Resonance, and XRD study was carried out in the X-ray Diffraction Centre (St. Petersburg State University).

ABBREVIATIONS

tetrahydrothiophene = THT
N,*N*′-dicyclohexylcarbodiimide = DCCI
human serum albumin = HSA
antibodies against HSA produced in rabbit = anti-HSA antibodies
α-chymotrypsinfrom bovine pancreas = ACHT
soybean trypsin inhibitor = SBTI
N-benzoyl-L-tyrosine ethyl ester = BTEE
N-benzoyl-L-arginine *p*-nitroanilide hydrochloride = BAPNA
1,4-bis(diphenylphosphino)benzene = dppb

REFERENCES

(1) Baggaley, E.; Weinstein, J. A.; Williams, J. A. G. *Coord. Chem. Rev.* **2012**, *256*, 1762−1785.
(2) Thorp-Greenwood, F. L.; Balasingham, R. G.; Coogan, M. P. *J. Organomet. Chem.* **2012**, *714*, 12−21.
(3) Thorp-Greenwood, F. L. *Organometallics* **2012**, *31*, 5686−5692.
(4) Lo, K. K.-W.; Choi, A. W.-T.; Law, W. H.-T. *Dalton Trans.* **2012**, *41*, 6021−6047.
(5) Zhao, Q.; Huang, C.; Li, F. *Chem. Soc. Rev.* **2011**, *40*, 2508−2524.
(6) Lakowicz, J. R. *Principles of fluorescence spectroscopy*; Springer: New York, 2009.
(7) Mizukami, S.; Yamamoto, T.; Yoshimura, A.; Watanabe, S.; Kikuchi, K. *Angew. Chem., Int. Ed.* **2011**, *50*, 8750−8752.
(8) Leung, S.-K.; Liu, H.-W.; Lo, K. K.-W. *Chem. Commun.* **2011**, *47*, 10548−10550.
(9) Dattelbaum, J. D.; Abugo, O. O.; Lakowicz, J. R. *Bioconjugate Chem.* **2000**, *11*, 533−536.
(10) Ferri, E.; Donghi, D.; Panigati, M.; Prencipe, G.; D'Alfonso, L.; Zanoni, I.; Baldoli, C.; Maiorana, S.; D'Alfonso, G.; Licandro, E. *Chem. Commun.* **2010**, *46*, 6255−6257.

(11) Lau, J. S.-Y.; Lee, P.-K.; Tsang, K. H.-K.; Ng, C. H.-C.; Lam, Y.-W.; Cheng, S.-H.; Lo, K. K.-W. *Inorg. Chem.* **2009**, *48*, 708−718.
(12) Lo, K. K. W.; Li, C. K.; Lau, K. W.; Zhu, N. Y. *Dalton Trans.* **2003**, 4682−4689.
(13) Lo, K. K. W.; Chung, C. K.; Lee, T. K. M.; Lui, L. H.; Tsang, K. H. K.; Zhu, N. Y. *Inorg. Chem.* **2003**, *42*, 6886−6897.
(14) Wang, Y.; Wang, X.; Wang, J.; Zhao, Y.; He, W.; Guo, Z. *Inorg. Chem.* **2011**, *50*, 12661−12668.
(15) Liu, Y.; Yu, Q.; Wang, C.; Sun, D.; Huang, Y.; Zhou, Y.; Liu, J. *Inorg. Chem. Commun.* **2012**, *24*, 104−109.
(16) Samari, F.; Hemmateenejad, B.; Shamsipur, M.; Rashidi, M.; Samouei, H. *Inorg. Chem.* **2012**, *51*, 3454−3464.
(17) Siu, P. K. M.; Ma, D. L.; Che, C. M. *Chem. Commun.* **2005**, 1025−1027.
(18) Tabassum, S.; Al-Asbahy, W. M.; Afzal, M.; Arjmand, F. *J. Photochem. Photobiol., B* **2012**, *114*, 132−139.
(19) Wang, X.; Wang, X.; Wang, Y.; Guo, Z. *Chem. Commun.* **2011**, *47*, 8127−8129.
(20) Yousefi, R.; Aghevlian, S.; Mokhtari, F.; Samouei, H.; Rashidi, M.; Nabavizadeh, S. M.; Tavaf, Z.; Pouryasin, Z.; Niazi, A.; Faghihi, R.; Papari, M. M. *Appl. Biochem. Biotechnol.* **2012**, *167*, 861−872.
(21) Lo, K. K.-W.; Li, S. P.-Y.; Zhang, K. Y. *New J. Chem.* **2011**, *35*, 265−287.
(22) Koshevoy, I. O.; Lin, Y.-C.; Karttunen, A. J.; Chou, P.-T.; Vainiotalo, P.; Tunik, S. P.; Haukka, M.; Pakkanen, T. A. *Inorg. Chem.* **2009**, *48*, 2094−2102.
(23) Koshevoy, I. O.; Karttunen, A. J.; Tunik, S. P.; Haukka, M.; Selivanov, S. I.; Melnikov, A. S.; Serdobintsev, P. Y.; Pakkanen, T. A. *Organometallics* **2009**, *28*, 1369−1376.
(24) Koshevoy, I. O.; Lin, Y.-C.; Karttunen, A. J.; Haukka, M.; Chou, P.-T.; Tunik, S. P.; Pakkanen, T. A. *Chem. Commun.* **2009**, 2860−2862.
(25) Koshevoy, I. O.; Lin, Y.-C.; Chen, Y.-C.; Karttunen, A. J.; Haukka, M.; Chou, P.-T.; Tunik, S. P.; Pakkanen, T. A. *Chem. Commun.* **2010**, *46*, 1440−1442.
(26) Koshevoy, I. O.; Karttunen, A. J.; Tunik, S. P.; Janis, J.; Haukka, M.; Melnikov, A. S.; Serdobintsev, P. Y.; Pakkanen, T. A. *Dalton Trans.* **2010**, *39*, 2676−2683.
(27) Dereza, P. Y.; Krytchankou, I. S.; Krupenya, D. V.; Gurzhiy, V. V.; Koshevoy, I. O.; Melnikov, A. S.; Tunik, S. P. *Z. Anorg. Allg. Chem.* **2013**, *639*, 398−402.
(28) Baldwin, R. A.; Cheng, M. T. *J. Org. Chem.* **1967**, *32*, 1572−1577.
(29) Uson, R.; Laguna, A.; Laguna, M. *Inorg. Synth.* **1989**, *26*, 85−91.
(30) Kubas, G. J. *Inorg. Synth.* **1979**, *19*, 90−92.
(31) Sheldrick, G. M. *Acta Crystallogr., Sect. A: Found. Crystallogr.* **2008**, *64*, 112−122.
(32) Dolomanov, O. V.; Bourhis, L. J.; Gildea, R. J.; Howard, J. A. K.; Puschmann, H. *J. Appl. Crystallogr.* **2009**, *42*, 339−341.
(33) Sheldrick, G. M. *SADABS*; University of Gottingen: Gottingen, Germany, 2004.
(34) Ponomareva, E. A.; Kartuzova, V. E.; Vlakh, E. G.; Tennikova, T. B. *J. Chromatogr., B: Anal. Technol. Biomed. Life Sci.* **2010**, *878*, 567−574.
(35) Ravnsbaek, J. B.; Jacobsen, M. F.; Rosen, C. B.; Voigt, N. V.; Gothelf, K. V. *Angew. Chem., Int. Ed.* **2011**, *50*, 10851−10854.
(36) Hermanson, G. T. In *Bioconjugate Techniques*, 2nd ed.; Academic Press: New York, 2008; pp 169−212.
(37) Shakirova, J. R.; Grachova, E. V.; Gurzhiy, V. V.; Koshevoy, I. O.; Melnikov, A. S.; Sizova, O. V.; Tunik, S. P.; Laguna, A. *Dalton Trans.* **2012**, *41*, 2941−2949.
(38) Koshevoy, I. O.; Karttunen, A. J.; Tunik, S. P.; Haukka, M.; Selivanov, S. I.; Melnikov, A. S.; Serdobintsev, P. Y.; Khodorkovskiy, M. A.; Pakkanen, T. A. *Inorg. Chem.* **2008**, *47*, 9478−9488.
(39) Koshevoy, I. O.; Lin, C.; Karttunen, A. J.; Jänis, J.; Haukka, M.; Tunik, S. P.; Chou, P.; Pakkanen, T. A. *Chem.—Eur. J.* **2011**, *17*, 11456−11466.
(40) Koshevoy, I. O.; Koskinen, L.; Haukka, M.; Tunik, S. P.; Serdobintsev, P. Y.; Melnikov, A. S.; Pakkanen, T. A. *Angew. Chem., Int. Ed.* **2008**, *47*, 3942−3945.
(41) He, X.; Zhu, N.; Yam, V. W.-W. *Dalton Trans.* **2011**, *40*, 9703−9710.
(42) Manbeck, G. F.; Brennessel, W. W.; Stockland, R. A.; Eisenberg, R. *J. Am. Chem. Soc.* **2010**, *132*, 12307−12318.
(43) Fischer, M. J. E. In *Surface Plasmon Resonance (Methods in Molecular Biology)*; Mol, N. J., Fischer, M. J. E., Eds.; Humana Press: New York, 2010; pp 55−73.
(44) Koshevoy, I. O.; Smirnova, E. S.; Domenech, A.; Karttunen, A. J.; Haukka, M.; Tunik, S. P.; Pakkanen, T. A. *Dalton Trans.* **2009**, 8392−8398.
(45) Benčina, M.; Benčina, K.; Štrancar, A.; Podgornik, A. *J. Chromatogr., A* **2005**, *1065*, 83−91.
(46) Uygun, M.; Uygun, D. A.; Özçalışkan, E.; Akgöl, S.; Denizli, A. *J. Chromatogr., B: Anal. Technol. Biomed. Life Sci.* **2012**, *887−888*, 73−78.
(47) Sharma, P.; Nath, A. K.; Kumari, R.; Bhardwaj, S. V. *J. For. Res. (Engl. Ed.)* **2012**, *23*, 131−137.